Generalised dq-dynamic phasor modelling of a STATCOM connected to a grid for stability analysis

Khaled Abojlala, Grain Asad, Khaled Ahmed, Derrick Holliday, Lie Xu
Electrical and electronic engineering department, University of Strathclyde, Glasgow, United Kingdom
*Khaled.Abojlala@Strath.ac.uk

Abstract: The synchronous dq based small-signal stability using the eigenvalue analysis and impedance methods is widely employed to assess system stability. Generally, the harmonics are ignored in stability analysis which may lead to inaccuracies in stability predictions, particularly, when the system operates in a harmonic-rich environment. Typically, the harmonic state-space method (HSS) facilitates stability studies of linear time-periodic (LTP) systems, which considers the impact of harmonics. The use of the dq-dynamic phasor state space and impedance method offers significant advantages over the HSS counterpart, as it reduces system order, is more suitable for studying control systems, retains mutual coupling of harmonics, and simplifies the stability study under unbalanced conditions. This paper extends dynamic phasor modelling for studying stability of modern power systems that include power converters. It is shown that the proposed method reproduces the typical response of STATCOM at the fundamental frequency as well as at significant low-order harmonics using both eigenvalues and impedance analysis. Quantitative validations of the proposed extended models against synchronous dq small signal models confirm their validity.

Acronyms and definitions

C_{dc}	STATCOM dc side capacitor
h	Harmonic order.
i_{dc}	STATCOM dc link current
$\mathbf{i_{sdq}}$	STATCOM Direct and quadrature currents vector
k	An integer number representing harmonic order, which is the axis to which referred
K_{pdq}	STATCOM controller proportional gains
K_{idq}	STATCOM controller integral gains
$\mathcal{L}_a, \mathcal{L}_b$	The number of states and inputs of the studied system
$\mathbf{L_{dq}}$	Return ratio matrix of grid-load
R_f, L_f	STATCOM resistance and inductance
v_{dc}	STATCOM dc link voltage
$\mathbf{v_{dqk}}$	Direct and quadrature voltages vector at k^{th} harmonic
$X_k(t)$	A function of time representing the complex Fourier coefficient 'dynamic phasor parameter' of the periodic signal
$\boldsymbol{\varepsilon_k}$	Coupling impedance caused by harmonic k at fundamental frequency.
$\boldsymbol{\mu_{k,0}}$	Coupling impedance caused by the fundamental frequency at harmonic k
$\boldsymbol{\rho}$	A coupling impedance which caused by the existence of positive and negative harmonics at a specific harmonic

1. Introduction

The existence of harmonics and oscillations over a wide range of frequencies represent major problems for the reliable operation of power systems. These harmonics and oscillations could be initiated by different events in the power system. For example, low-frequency oscillations can be initiated due to sub-synchronous resonance (SSR), whilst high-frequency variations are largely initiated by switching of power electronics converters [1][2]. Many stability studies ignore these variations in their modelling and analyse system performance based on the fundamental frequency only [3], [4]. However, this assumption could lead to an incorrect assessment of system stability [5][6]. Therefore, careful and detailed modelling of the power system components is essential when assessing stability in systems that contain significant harmonics or unbalance.

Typical stability studies are carried out based on a set of equations that model systems in a specific domain. For example, the synchronous dq approach has been employed to study the dc-link variation of HVDC systems [7], and a VSC connected to a weak grid [8]. Also, synchronous dq impedance models were successfully implemented in the application of detecting system oscillations [9][10], and retuning of controllers for improved damping [11]–[15]. Although this modelling method is suitable for control systems and can be linearised with insignificant error, it is limited for fundamental frequency analysis using a single coordinate. Similarly an equivalent stationary-frame ($\alpha\beta$) impedance model has been introduced [16]. In one application, the $\alpha\beta$ model was used to simplify the stability assessment of a VSC based system by converting the system into a single-input-single-output system as a positive and negative sequence system [17]. However, ignoring the frequency coupling between the sequence quantities may affect the results of analysing large systems where coupling is usually present. This disadvantage [17] has been addressed [18][19] by taking into consideration the coupling between the positive sequence and negative sequence quantities. The capability of this modelling technique was limited for frequencies more than twice the fundamental frequency [20], cannot include harmonics and its oscillatory nature is not suitable for small-signal studies. The inclusion of harmonics in stability studies was introduced using the harmonic linearisation and Harmonic State Space (HSS) methods. The former method was employed to design control systems of VSC based FACTS devices and study their interactions with other system

components [21]–[26]. Even though the harmonic linearisation method can reveal the frequency coupling between the positive and negative sequence quantities, the imposition of the linear time invariant (LTI) property compromises its capacity to predict the coupling that might occur between existing harmonics [20]. HSS can, however, include harmonics and present their effect on system response, by mapping the input and output signals in linear time-periodic (LTP) systems using the harmonic transfer function (HTF) [27]–[29] linear operator. The HSS approach has been employed for modelling balanced and unbalanced operation of VSC-FACTS devices and their stability [30]–[32]. High-order matrices and time-variant parameters are, however, the main disadvantages of this method.

Dynamic phasor (DP) modelling helps with the inclusion of harmonics and the investigation of unbalance and converts the periodic parameters to dc parameters which improves the accuracy of system linearisation. Most of the implementations of dynamic phasor modelling for stability assessment were carried out using the abc-dynamic phasor. Such an approach increases the number of equations and variables required to be analysed, and sometimes per-phase models were used to simplify the analysis. However, the per-phase models are not suitable for the study of unbalanced systems. However, the aforementioned per-phase modelling has several advantages compared with conventional the dq equivalent [33]. The per-phase model has been employed to design a solid-state transformer controller in the presence of disturbances using state-space analysis, identify low-frequency oscillations in series compensated systems, and study the effect of phase unbalance on system oscillations [34][35]. Similarly, the small-signal impedance model based on the single-phase dynamic phasor was utilised to identify the causes of sub-synchronous resonance (SSR), but this formulation led to diagonal and off-diagonal impedances that were entirely fictitious and had no physical meaning [36]. One reported stability assessment [37] artificially accounts for fundamental frequency and second harmonic in the ac and dc sides respectively.

This paper presents a generalised dq-dynamic phasor (GDQ-DP) small-signal stability model suitable for both electromagnetic transients and electromechanical dynamics, including harmonic stability. The proposed model retains the attributes of the synchronous dq model, i.e. linear time-invariant (LTI), which is convenient for stability studies. The impedance model derived from the proposed GDQ-DP model facilitates stability studies under balanced and unbalanced conditions using well-established stability criteria. One-to-one comparison of the proposed extended model and conventional synchronous dq confirms its validity and reveals its capacity to assess stability under unbalanced and harmonic polluted conditions.

The paper comprises eight sections. Sections 2 and 3 review the basics of dynamic phasor and synchronous dq modelling, using STATCOM as an example. Sections 4 and 5 develop a generalised dq-DP model and introduce criteria for stability assessment when eigenvalue analysis and small-signal impedance are employed. The effectiveness of the proposed model for predicting stability of balanced and unbalanced systems is tested in Section 6. High-level qualitative comparisons between the proposed model and other conventional modelling techniques are presented in Section 7. The main findings and observations are highlighted in Section 8. It is important to stress that the main intension of this paper is development of a generalised dynamic phasor model readily available for use in balanced and unbalanced systems, and ac grids with significant harmonic content. Controlling a specific sequence or harmonics is not the focus of this research.

2. Conventional dynamic phasor modelling

This section reviews the fundamentals of dynamic phasor modelling and its merits when applied to power systems. Generally, DP defines a real value waveform $x(\tau)$ during the interval $\tau \in (t-T, t)$ using Fourier series [38]:

$$x(\tau) = \sum_{k=-\infty}^{\infty} \overrightarrow{\mathbf{X_k}(t)} e^{jk\omega_s \tau} \tag{1}$$

The time-variant Fourier coefficient $\left(\overrightarrow{\mathbf{X_k}(t)}\right)$ is called a dynamic phasor, and can be determined at time (t) from (2):

$$\overrightarrow{\mathbf{X_k}(t)} = \frac{1}{T}\int_{t-T}^{t} x(\tau) e^{-jk\omega_s \tau} d\tau = \langle x \rangle_k \tag{2}$$

A DP, with harmonics included, can be used to represent a generic dq quantity:

$$\begin{aligned} \vec{\mathbf{V}} &= v_d + jv_q = \frac{2}{3}(v_a + a^2 v_b + a v_c) e^{jn\omega_s t} \\ &= \left(v_{dk} + jv_{qk}\right) + \sum_{\substack{n=-\infty \\ n\neq k}}^{\infty} \left(v_{dk} + jv_{qk}\right) e^{j(n-k)\omega t} \end{aligned} \tag{3}$$

where k is an integer number representing harmonic order, which is the axis to which the quantities are referred.

By using (3), the measured quantities are transformed to dq frame at each harmonic of interest (k), and then the undesirable harmonics $(\forall n, n \neq k)$ are filtered out using low-pass filter as shown in Fig. 1 In this way, any quantity expressed in the abc frame can be transformed into positive and negative sequence dq components and then to the DP representation.

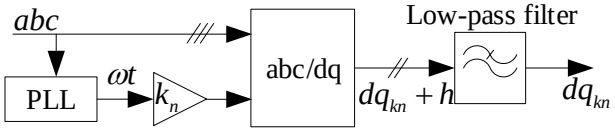

Fig. 1. Extraction of dynamic phasor parameters.

3. Synchronous dq modelling

In this section, the synchronous dq modelling of a STATCOM is used to demonstrate the proposed dq-dynamic phasor modelling technique.

The basic topology of a STATCOM connected to a power network is illustrated in Fig.2 a. Fig.2b depicts the STATCOM cascaded control loops employed in this paper for illustration [39][40]. The outer controllers on d and q axes regulate dc voltage and reactive power respectively, while the inner controllers regulate the dq current and estimate the modulating signals.

In this paper, the system or ac grid voltage at the point-of-common-coupling (PCC) is assumed to be the reference and aligned with the dq frame. For simplicity, it is assumed that the ac grid is strong, and that the PLL dynamics can be ignored without introducing error or compromising the generality of the proposed model. Also, the pulse width modulation (PWM) delay and the measurement delay are ignored in the analysis.

Based on the current directions assumed in Fig.2a, the current equation of the STATCOM power circuit can be written as (4) and (5) [41]:

$$\frac{\mathbf{d}}{\mathbf{dt}}\mathbf{\Delta i_{sdq}} = \frac{1}{L_f}\mathbf{\Delta x_{12}} - \left(\frac{R_f}{L_f} - \gamma(\omega) + \frac{K_{pidq}}{L_f}\right)\mathbf{\Delta i_{sdq}} + \frac{1}{L_f}\mathbf{\Delta v_{sdq}} + \frac{K_{pidq}}{L_f}\mathbf{\Delta i^*_{sdq}} \quad (4)$$

$$\frac{\mathbf{d}}{\mathbf{dt}}\mathbf{\Delta x_{12}} = K_{iidq}\left(\mathbf{\Delta i^*_{sdq}} - \mathbf{\Delta i_{sdq}}\right) \quad (5)$$

The reference currents are given by:

$$\mathbf{\Delta i^*_{sdq}} = K_{pvdq}(\mathbf{\Delta v^*} - \mathbf{\Delta v}) + \mathbf{\Delta x_{34}} \quad (6)$$

Considering the power balance between the ac and dc sides, the linearised equation describing dc voltage dynamics is:

$$\frac{\mathrm{d}}{\mathrm{dt}}\Delta v_{dc} = \frac{1}{C_{dc}v_{dc}}\left\{\frac{3}{2}\left(\mathbf{i^T_{sdq}}.\mathbf{\Delta v_{sdq}} + \mathbf{v^T_{sdq}}.\mathbf{\Delta i_{sdq}}\right) - 2i_{sd}.R_f\Delta i_{sd} + \frac{1}{C_{dc}v_{dc}}\left(i^2_{sd}.R_f - \frac{3}{2}\mathbf{v^T_{sdq}}.\mathbf{i_{sdq}}\right)\Delta v_{dc}\right\} \quad (7)$$

The linearised form of reactive power is given as:

$$\Delta Q = \frac{3}{2}\mathbf{\Delta i^T_{sdq}}\begin{bmatrix}-\Delta v_{sq}\\ \Delta v_{sd}\end{bmatrix} + \frac{3}{2}\mathbf{\Delta v^T_{sdq}}\begin{bmatrix}-\Delta i_{sq}\\ \Delta i_{sd}\end{bmatrix} \quad (8)$$

$$\frac{\mathbf{d}}{\mathbf{dt}}\mathbf{\Delta x_{34}} = K_{ivdq}(\mathbf{\Delta v^*} - \mathbf{\Delta v}) \quad (9)$$

Superscript * denotes reference quantities, K_{pdq},K_{idq} are the proportional and integral controller gains, $\gamma = \begin{bmatrix}0 & 1\\ -1 & 0\end{bmatrix}$, $\mathbf{x_{lm}} = [x_l \quad x_m]^T$, $\mathbf{v_{sdq}} = [v_{sd} \quad v_{sq}]^T$, $\mathbf{i_{sdq}} = [i_{sd} \quad i_{sq}]^T$ and $\mathbf{v} = [v_{dc} \quad \mathrm{Q}]^T$.

Rearranging (4) to (9), the overall state-space equation of the STATCOM in the dq frame is:

$$\frac{\mathbf{d}}{\mathbf{dt}}\mathbf{\Delta X} = \mathbf{A_{dq}}\mathbf{\Delta X} + \mathbf{B_{dq}}\mathbf{\Delta U} \quad (10)$$

$$\mathbf{\Delta i_{sdq}} = \mathbf{C_{dq}}\mathbf{\Delta X} \quad (11)$$

where the state, input and output matrices, and vectors are defined as:

$$\mathbf{\Delta X} = [\Delta x_1 \quad \Delta x_2 \quad \Delta x_3 \quad \Delta x_4 \quad \mathbf{\Delta i_{sdq}} \quad \Delta v_{dc}]^T$$

$$\mathbf{\Delta U} = [\Delta v_{sd} \quad \Delta v_{sq} \quad \Delta v^*_{dc} \quad \mathrm{Q}^*]^T$$

$$\alpha_{dc} = i^2_{sd}.R_f - \frac{3}{2}(v_{sd}.i_{sd} + v_{sq}.i_{sq})$$

$$\mathbf{B_{dq}} = \begin{bmatrix} 0 & 0 & K_{iid}K_{pvd} & 0 \\ \frac{3K_{iiq}K_{pvq}i_{sq}}{2} & \frac{-3K_{iiq}K_{pvq}i_{sd}}{2} & 0 & K_{iiq}K_{pvq} \\ 0 & 0 & K_{ivd} & 0 \\ \frac{3K_{ivq}i_{sq}}{2} & \frac{-3K_{ivq}i_{sd}}{2} & 0 & K_{ivq} \\ \frac{1}{L_f} & 0 & \frac{K_{pid}K_{pvd}}{L_f} & 0 \\ \frac{3K_{piq}K_{pvq}i_{sq}}{2L_f} & \frac{1-\frac{3}{2}K_{piq}K_{pvq}i_{sd}}{L_f} & 0 & \frac{K_{piq}}{L_f} \\ \frac{3i_{sd}}{2C_{dc}v_{dc}} & \frac{3i_{sq}}{2C_{dc}v_{dc}} & 0 & 0 \end{bmatrix}$$

$$\mathbf{A_{dq}} = \begin{bmatrix} 0 & 0 & K_{iid} & 0 & -K_{iid} & 0 & -K_{iid}K_{pvd} \\ 0 & 0 & 0 & K_{iiq} & -\frac{3}{2}K_{iiq}K_{pvq}v_{sq} & \frac{3}{2}K_{iiq}K_{pvq}v_{sd} - K_{iiq} & 0 \\ 0 & 0 & 0 & 0 & 0 & 0 & -K_{ivd} \\ 0 & 0 & 0 & 0 & -\frac{3}{2}K_{ivq}v_{sq} & \frac{3}{2}K_{ivq}v_{sd} & 0 \\ \frac{1}{L_f} & 0 & \frac{K_{pid}}{L_f} & 0 & \frac{-R_f-K_{pid}}{L_f} & \omega & -\frac{K_{pid}K_{pvd}}{L_f} \\ 0 & \frac{1}{L_f} & 0 & \frac{K_{piq}}{L_f} & -\frac{\frac{3}{2}K_{piq}K_{pvq}v_{sq}}{L_f} - \omega & \frac{-R_f-K_{piq}+\frac{3}{2}K_{piq}K_{pvq}v_{sd}}{L_f} & 0 \\ 0 & 0 & 0 & 0 & \frac{\frac{3}{2}v_{sd}-2i_{sd}.R_f}{C_{dc}v_{dc}} & \frac{\frac{3}{2}v_{sq}}{C_{dc}v_{dc}} & \frac{\alpha_{dc}}{C_{dc}v^2_{dc}} \end{bmatrix}$$

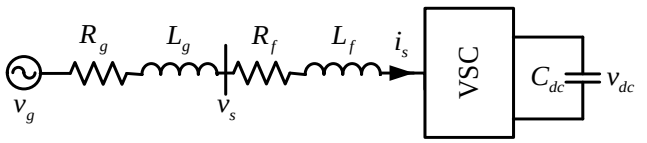

(a)

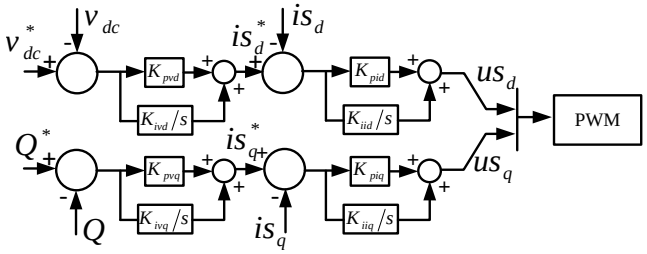

(b)

Fig.2. STATCOM construction and control:**(a)** Simplified diagram of grid-connected STATCOM, **(b)** control system.

State-space equations (10) and (11) permit asymptotic stability assessment of complex systems using eigenvalues. The derived state-space model has seven states, which are the STATCOM dq currents and auxiliary states that represent the integral parts of the current controllers, and the dc-link voltage and auxiliary states associated with the integral parts of the dc voltage and reactive power controllers. The model also has four inputs, which are the ac grid dq voltages, and the dc-link voltage and reactive power commands. The small-signal impedance approach offers a powerful and practical alternative method for stability assessment, where synthesis of detailed system model is challenging [11][42]. The small-signal impedance model can be extracted directly from the standard state-space model described in (10) and (11). Following minor algebraic manipulation (particularly, expressing the system voltages in terms of the currents), yields:

$$\mathbf{\Delta v_{sdq}} = \mathbf{a_z \Delta i_{sdq}} - \mathbf{b_z \Delta i^*_{sdq}} \tag{12}$$

$$\mathbf{\Delta i^*_{sdq}} = \mathbf{c_z}(\mathbf{\Delta v^*} - \mathbf{\Delta v}) \tag{13}$$

$$\mathbf{d_z \Delta v} = \mathbf{e_z \Delta v_{sdq}} + \mathbf{f_z \Delta i_{sdq}} \tag{14}$$

On this basis, the small signal impedance model of the STATCOM becomes:

$$\mathbf{\Delta v_{sdq}} = \mathbf{Z_{dq} \Delta i_{sdq}} - \mathbf{b_z c_z \Delta v^*} \tag{15}$$

where $\mathbf{Z_{dq}}$ represents STATCOM impedance matrix in the dq reference frame, and is given by:

$$\mathbf{Z_{dq}} = (\mathbf{I} - \mathbf{b_z c_z d_z^{-1} f_z})^{-1}(\mathbf{a_z} + \mathbf{b_z c_z d_z^{-1} e_z}) \tag{16}$$

Equation (16) is simplified as:

$$\mathbf{Z_{dq}} = \begin{bmatrix} \frac{\Delta v_{sd}}{\Delta i_{sd}} & \frac{\Delta v_{sd}}{\Delta i_{sq}} \\ \frac{\Delta v_{sq}}{\Delta i_{sd}} & \frac{\Delta v_{sq}}{\Delta i_{sq}} \end{bmatrix} = \begin{bmatrix} Z_{dd} & Z_{dq} \\ Z_{qd} & Z_{qq} \end{bmatrix} \tag{17}$$

The matrices in (16) are defines as:

$$\mathbf{a_z} = \begin{bmatrix} L_f s + R_f + \left(K_{pid} + \frac{K_{iid}}{s}\right) & -\omega L_f \\ \omega L_f & L_f s + R_f + \left(K_{ipq} + \frac{K_{iiq}}{s}\right) \end{bmatrix}$$

$$\mathbf{b_z} = \begin{bmatrix} K_{pid} + \frac{K_{iid}}{s} & 0 \\ 0 & K_{ipq} + \frac{K_{iiq}}{s} \end{bmatrix}, \mathbf{d_z} = \begin{bmatrix} \frac{sC_{dc}v_{dc}^2 - \alpha_{dc}}{v_{dc}} & 0 \\ 0 & 1 \end{bmatrix}$$

$$\mathbf{c_z} = \begin{bmatrix} K_{pvd} + \frac{K_{ivd}}{s} & 0 \\ 0 & K_{pvq} + \frac{K_{ivq}}{s} \end{bmatrix} \mathbf{f_z} = \frac{3}{2}\begin{bmatrix} i_{sd} & i_{sq} \\ -i_{sq} & i_{sd} \end{bmatrix}$$

$$\mathbf{e_z} = \begin{bmatrix} \frac{3}{2}v_{sd} - 2R_f i_{sd} & \frac{3}{2}v_{sq} \\ \frac{3}{2}v_{sq} & -\frac{3}{2}v_{sd} \end{bmatrix}$$

4. Generalised dq-dynamic phasor modelling for stability analysis

This section proposes a generalised model that can facilitate stability studies, where the effects of harmonics and network unbalance are considered. For illustration, the STATCOM synchronous dq model described in Section 2 is transformed to the dq-dynamic phasor model. Thus, the dynamic phasor transformations of the state-space equations (10) and (11) become:

$$\frac{\mathbf{d}}{\mathbf{dt}}\langle \mathbf{\Delta X} \rangle_k = \sum_{k=-\infty}^{\infty} \langle \mathbf{A_{dq} \Delta X} \rangle_k + \sum_{k=-\infty}^{\infty} \langle \mathbf{B_{dq} \Delta U} \rangle_k \tag{18}$$

$$\langle \mathbf{\Delta i_{sdq}} \rangle_k = \sum_{k=-\infty}^{\infty} \langle \mathbf{C_{dq} \Delta X} \rangle_k \tag{19}$$

The expansion of (18) and (19) can be carried out using previously described dynamic phasor characteristics [38]. These equations represent generalised state-space equations with infinite dimensions which can be written in compact form as:

$$\frac{\mathbf{d}}{\mathbf{dt}}\mathbf{\Delta X_k} = \mathbf{A_{DP} \Delta X_k} + \mathbf{B_{DP} \Delta U}_k \tag{20}$$

$$\langle \mathbf{\Delta i_{sdq}} \rangle_k = \mathbf{C_{DP} \Delta X_k} \tag{21}$$

where the state and input matrices and vectors have infinite length and are given in a general form as:

$$\mathbf{\Delta X}_\mathrm{k} = [\mathbf{\Delta X}_{k=0} \quad \mathbf{\Delta X}_{k=k_1} \quad \mathbf{\Delta X}_{k=-k_1} \quad \ldots \quad \mathbf{\Delta X}_{k=-k_n}]^\mathrm{T}$$

$$\mathbf{\Delta U}_\mathrm{k} = [\langle \mathbf{\Delta U} \rangle_{k=0} \ \langle \mathbf{\Delta U} \rangle_{k=k_1} \ \langle \mathbf{\Delta U} \rangle_{k=-k_1} \ \ldots \ \langle \mathbf{\Delta U} \rangle_{k=-k_n}]^\mathrm{T}$$

The matrices ($\mathbf{A_{DP}}, \mathbf{B_{DP}}$ and $\mathbf{C_{DP}}$) are time invariant matrices which have sets of submatrices that can include the harmonics of the studied system.

$$\mathbf{A_{DP}}=\begin{bmatrix} \mathbf{a_{k=0}} & \mathbf{ac_{k=-k_1}} & \mathbf{ac_{k=k_1}} & \cdots & \mathbf{ac_{k=-k_n}} & \mathbf{ac_{k=k_n}} \\ \mathbf{ac_{k=k_1}} & \mathbf{a_{k=k_1}} & & & \mathbf{0} & \mathbf{0} \\ \mathbf{ac_{k=-k_1}} & & \mathbf{a_{k=-k_1}} & & \mathbf{0} & \mathbf{0} \\ \vdots & & & \ddots & & \vdots \\ & \mathbf{0} & \mathbf{0} & & \mathbf{a_{k=k_n}} & \\ \mathbf{ac_{k=-k_n}} & \mathbf{0} & \mathbf{0} & \cdots & & \mathbf{a_{k=-k_n}} \end{bmatrix}$$

$$\mathbf{B_{DP}}=\begin{bmatrix} \mathbf{b_{k=0}} & \mathbf{bc_{k=-k_1}} & \mathbf{bc_{k=k_1}} & \cdots & \mathbf{bc_{k=-k_n}} & \mathbf{bc_{k=k_n}} \\ \mathbf{bc_{k=k_1}} & \mathbf{b_{k=k_1}} & & & \mathbf{0} & \mathbf{0} \\ \mathbf{bc_{k=-k_1}} & & \mathbf{b_{k=-k_1}} & & \mathbf{0} & \mathbf{0} \\ \vdots & & & \ddots & & \vdots \\ \mathbf{bc_{k=k_n}} & \mathbf{0} & \mathbf{0} & & \mathbf{b_{k=kn}} & \\ \mathbf{bc_{k=-k_n}} & \mathbf{0} & \mathbf{0} & \cdots & & \mathbf{b_{k=-k_n}} \end{bmatrix}$$

The definitions of the sub-matrices of $(\mathbf{A_{DP}})$ and $(\mathbf{B_{DP}})$ are found in the Appendix. Equations (20) and (21) are capable of including the fundamental frequency ($k=0$) as well as an infinite number of harmonics ($k=\mp\infty$). Each harmonic frequency 'except the fundamental frequency' generates two components: the positive and negative sequence components of the kth harmonic (depicted by suffixes k and $-k$). The existence of the positive and negative sequence components in (20) and (21) facilitate stability studies of balanced systems, while the expansion of the fundamental frequency represents unbalanced systems.

In the generalised state matrix $(\mathbf{A_{DP}})$, matrices $\left(\mathbf{ac_{k=-k_1}}\right)$ and $\left(\mathbf{ac_{k=k_1}}\right)$ represent the effects of positive and negative sequence components on the fundamental frequency, and the coupling of the fundamental frequency on the positive and negative components.

The size of the state and input matrices $(\mathbf{A_{DP}},\mathbf{B_{DP}})$ is calculated using (22) for the state matrix and (23) for the input matrix as follows:

$$size(\mathbf{A_{DP}})=(2(1+n)\mathcal{L}_a,2(1+n)\mathcal{L}_a) \quad (22)$$

$$size(\mathbf{B_{DP}})=(2(1+n)\mathcal{L}_a,2(1+n)\mathcal{L}_b) \quad (23)$$

where n is the number of harmonics to be included in the study, and $\mathcal{L}_a$ and $\mathcal{L}_b$ represent the number of states and inputs of the studied system. For example, when two harmonics and the fundamental are considered when analysing STATCOM stability, the sizes of the state and input matrices $(\mathbf{A_{DP}})$ and $(\mathbf{B_{DP}})$ become (42×42) and (42×24) respectively.

In summary, the eigenvalues of the generalised state-space model presented in (20) and (21) can be employed to assess the stability of arbitrary power systems.

Similarly, the generalised impedance model of the STATCOM is derived from (12) to (14) as:

$$\sum_{k=-\infty}^{\infty}\langle\mathbf{\Delta v_{sdq}}\rangle_k=\sum_{-\infty}^{\infty}\langle\mathbf{a_z\Delta i_{sdq}}\rangle_k+\sum_{-\infty}^{\infty}\langle\mathbf{b_z\Delta i^*_{sdq}}\rangle_k \quad (24)$$

$$\sum_{k=-\infty}^{\infty}\langle\mathbf{\Delta i^*_{sdq}}\rangle_k=\sum_{k=-\infty}^{\infty}\langle\mathbf{c_z v^*}\rangle_k-\sum_{k=-\infty}^{\infty}\langle\mathbf{c_z\Delta v}\rangle_k \quad (25)$$

$$\sum_{k=-\infty}^{\infty}\langle\mathbf{d_z\Delta v}\rangle_k=\sum_{-\infty}^{\infty}\langle\mathbf{e_z\Delta v_{sdq}}\rangle_k+\sum_{-\infty}^{\infty}\langle\mathbf{f_z\Delta i_{sdq}}\rangle_k \quad (26)$$

Expanding (25) to (26) and rearranging yields:

$$\langle\mathbf{\Delta v_{sdq}}\rangle_k=\mathbf{A_z}\langle\mathbf{\Delta i_{sdq}}\rangle_k+\mathbf{B_z\Delta i^*_{sdq}} \quad (27)$$

$$\langle\mathbf{\Delta i^*_{sdq}}\rangle_k=\mathbf{C_z}\langle\mathbf{v^*}\rangle_k-\mathbf{C_z}\langle\mathbf{\Delta v}\rangle_k \quad (28)$$

$$\mathbf{D_z}\langle\mathbf{\Delta v}\rangle_k=\mathbf{E_z}\langle\mathbf{\Delta v_{sdq}}\rangle_k+\mathbf{F_z}\langle\mathbf{\Delta i_{sdq}}\rangle_k \quad (29)$$

where, the voltage and current vectors are given as:

$$\langle\mathbf{\Delta v_{sdq}}\rangle_k=$$
$$[\langle\mathbf{\Delta v_{sdq}}\rangle_{k=0}\,\langle\mathbf{\Delta v_{sdq}}\rangle_{k=k_1}\,\langle\mathbf{\Delta v_{sdq}}\rangle_{k=-k_1}\ldots\langle\mathbf{\Delta v_{sdq}}\rangle_{k=-k_n}]^T$$

$$\langle\mathbf{\Delta i_{sdq}}\rangle_k=$$
$$[\langle\mathbf{\Delta i_{sdq}}\rangle_{k=0}\ \langle\mathbf{\Delta i_{sdq}}\rangle_{k=k_1}\ \langle\mathbf{\Delta i_{sdq}}\rangle_{k=-k_1}\ \ldots\ \langle\mathbf{\Delta i_{sdq}}\rangle_{k=-k_n}]^T$$

$$\langle\mathbf{\Delta v}\rangle_{\mathrm{k}}=[\langle\mathbf{\Delta v}\rangle_{k=0}\ \langle\mathbf{\Delta v}\rangle_{k=k_1}\ \langle\mathbf{\Delta v}\rangle_{k=-k_1}\ \cdots\ \langle\mathbf{\Delta v}\rangle_{k=-k_n}]^{\mathrm{T}}$$

After further manipulation of (27) to (29), the generalised STATCOM impedance model is obtained as:

$$\mathbf{Z_{DP}}=(\mathbf{I}-\mathbf{B_zC_zD_z^{-1}F_z})^{-1}(\mathbf{A_z}+\mathbf{B_zC_zD_z^{-1}E_z}) \quad (30)$$

The impedance matrices in (30) have infinite dimensions and follow the same pattern found in the derivation of the state-space equations in (20) to (21), which are summarised as follows:

$$\mathbf{A_z}=\begin{bmatrix} \mathbf{hd_{k=0}} & \mathbf{hl_{k=-k_1}} & \mathbf{hl_{k=k_1}} & \cdots & \mathbf{hl_{k=k_n}} \\ \mathbf{hl_{k=k_1}} & \mathbf{hd_{k=k_1}} & \mathbf{0} & & \mathbf{0} \\ \mathbf{hl_{k=-k_1}} & \mathbf{0} & \mathbf{hd_{k=-k_1}} & & \mathbf{0} \\ \vdots & \mathbf{0} & \mathbf{0} & \ddots & \mathbf{0} \\ \mathbf{hl_{k=-k_n}} & \mathbf{0} & \mathbf{0} & & \mathbf{hd_{k=-k_n}} \end{bmatrix}$$

$$\mathbf{B_z}=\begin{bmatrix} \mathbf{Bd_{k=0}} & \mathbf{Bl_{k=-k_1}} & \mathbf{Bl_{k=k_1}} & \cdots & \mathbf{Bl_{k=k_n}} \\ \mathbf{Bl_{k=k_1}} & \mathbf{Bd_{k=k_1}} & \mathbf{0} & & \mathbf{0} \\ \mathbf{Bl_{k=-k_1}} & \mathbf{0} & \mathbf{Bd_{k=-k_1}} & & \mathbf{0} \\ \vdots & \mathbf{0} & \mathbf{0} & \ddots & \mathbf{0} \\ \mathbf{Bl_{k=-k_n}} & \mathbf{0} & \mathbf{0} & & \mathbf{Bd_{k=-k_n}} \end{bmatrix}$$

$$\mathbf{C_z}=\begin{bmatrix} \mathbf{Cd_{k=0}} & \mathbf{Cl_{k=-k_1}} & \mathbf{Cl_{k=k_1}} & \cdots & \mathbf{Cl_{k=k_n}} \\ \mathbf{Cl_{k=k_1}} & \mathbf{Cd_{k=k_1}} & \mathbf{0} & & \mathbf{0} \\ \mathbf{Cl_{k=-k_1}} & \mathbf{0} & \mathbf{Cd_{k=-k_1}} & & \mathbf{0} \\ \vdots & \mathbf{0} & \mathbf{0} & \ddots & \mathbf{0} \\ \mathbf{Cl_{k=-k_n}} & \mathbf{0} & \mathbf{0} & & \mathbf{Cd_{k=-k_n}} \end{bmatrix}$$

$$\mathbf{D_z}=\begin{bmatrix} \mathbf{Dd_{k=0}} & \mathbf{Dl_{k=-k_1}} & \mathbf{Dl_{k=k_1}} & \cdots & \mathbf{Dl_{k=k_n}} \\ \mathbf{Dl_{k=k_1}} & \mathbf{Dd_{k=k_1}} & \mathbf{0} & & \mathbf{0} \\ \mathbf{Dl_{k=-k_1}} & \mathbf{0} & \mathbf{Dd_{k=-k_1}} & & \mathbf{0} \\ \vdots & \mathbf{0} & \mathbf{0} & \ddots & \mathbf{0} \\ \mathbf{Dl_{k=-k_n}} & \mathbf{0} & \mathbf{0} & & \mathbf{Dd_{k=-k_n}} \end{bmatrix}$$

$$\mathbf{E_z}=\begin{bmatrix} \mathbf{Ed_{k=0}} & \mathbf{El_{k=-k_1}} & \mathbf{El_{k=k_1}} & \cdots & \mathbf{El_{k=k_n}} \\ \mathbf{El_{k=k_1}} & \mathbf{Ed_{k=k_1}} & \mathbf{0} & & \mathbf{0} \\ \mathbf{El_{k=-k_1}} & \mathbf{0} & \mathbf{Ed_{k=-k_1}} & & \mathbf{0} \\ \vdots & \mathbf{0} & \mathbf{0} & \ddots & \mathbf{0} \\ \mathbf{El_{k=-k_n}} & \mathbf{0} & \mathbf{0} & & \mathbf{Ed_{k=-k_n}} \end{bmatrix}$$

$$\mathbf{F_z}=\begin{bmatrix} \mathbf{Fd_{k=0}} & \mathbf{Fl_{k=-k_1}} & \mathbf{Fl_{k=k_1}} & \cdots & \mathbf{Fl_{k=k_n}} \\ \mathbf{Fl_{k=k_1}} & \mathbf{Fd_{k=k_1}} & \mathbf{0} & & \mathbf{0} \\ \mathbf{Fl_{k=-k_1}} & \mathbf{0} & \mathbf{Fd_{k=-k_1}} & & \mathbf{0} \\ \vdots & \mathbf{0} & \mathbf{0} & \ddots & \mathbf{0} \\ \mathbf{Fl_{k=-k_n}} & \mathbf{0} & \mathbf{0} & & \mathbf{Fd_{k=-k_n}} \end{bmatrix}$$

These generalised matrices are capable of determining the STATCOM impedance at arbitrary frequency, $-\infty \le k \le +\infty$. At fundamental frequency, $\mathbf{Z_{DP}}$ can be obtained by setting $k=0$ in submatrices $\mathbf{A_z}$ through $\mathbf{F_z}$.

The frequency coupling observed in the presented generalised dq-dynamic phasor and STATCOM model, and any VSC based devices, is a reflection of the instantaneous power variations into the dc link [43]. The frequency coupling affects the STATCOM impedance in both magnitude and the phase.

The STATCOM impedance in (30) can be re-written as:

$$\mathbf{Z_{DP}}=\begin{bmatrix} \mathbf{Z_f} & \boldsymbol{\varepsilon}_{\mathbf{k=-k_1}} & \boldsymbol{\varepsilon}_{\mathbf{k=k_1}} & \cdots & \boldsymbol{\varepsilon}_{\mathbf{k=-k_n}} & \boldsymbol{\varepsilon}_{\mathbf{k=k_n}} \\ \boldsymbol{\mu}_{\mathbf{k_1,0}} & \mathbf{Z_{k=k_1}} & \mathbf{0} & & \mathbf{0} & \mathbf{0} \\ \boldsymbol{\mu}_{\mathbf{-k_1,0}} & \mathbf{0} & \mathbf{Z_{k=-k_1}} & & \mathbf{0} & \mathbf{0} \\ \vdots & & & \ddots & & \vdots \\ \boldsymbol{\mu}_{\mathbf{k_n,0}} & \mathbf{0} & \mathbf{0} & & \mathbf{Z_{k=k_n}} & \mathbf{0} \\ \boldsymbol{\mu}_{\mathbf{-k_n,0}} & \mathbf{0} & \mathbf{0} & \ldots & \mathbf{0} & \mathbf{Z_{k=-k_n}} \end{bmatrix} \quad (31)$$

Equation (31) is generalised and written in a compact form as:

$$\mathbf{Z_{DP}}=\begin{Bmatrix} \mathbf{z_f}|_{k=0}+\sum_{k=-\infty}^{\infty}(\boldsymbol{\varepsilon}_\mathbf{k}) & k=0 \\ \mathbf{z_f}|_{k=k}+\boldsymbol{\mu}_{\mathbf{k,0}} & k\neq 0 \end{Bmatrix} \quad (32)$$

where $\boldsymbol{\varepsilon}_\mathbf{k}$ is the coupling between the harmonics and the fundamental frequency, and matrices $\boldsymbol{\mu}_{\mathbf{k,0}}$ represents the coupling between the fundamental frequency and the harmonics. The frequency coupling might appear also in the diagonal impedance as the dc-link voltage will be affected by the presence of the positive and negative sequence components. If it is assumed that the derived system is a decoupled system, where the system is assumed as a multi-grids operated at different frequencies, the coupling matrices will be equal to zero.

According to the dynamic phasor transformation in (3), the measured impedance in the abc coordinate frame at a specific harmonic is equal to the impedance of its generated harmonics represented in dq-dynamic phasor form multiplied by the transformation factor ($e^{\pm jk\omega t}$). The roll-off nature, i.e. low-pass characteristics of the inductances and capacitors, results in reasonably sized matrices for the analysed system [44]. The optimum size of the STATCOM matrices can be found by scanning the frequency spectrum until the impedance does not change and the additional eigenvalues are displaced by ($\pm j\omega$) without any changes in their real parts. It should be noted that for system analysis for harmonic order ($k=0$), the generalised state-space and impedance models will be equal to the forms of the synchronous dq model presented in Section 3.

Although the modelling process presented is carried out for a STATCOM, it is not limited to STATCOMs and can be generalised for modelling other system components.

5. Stability criteria of the proposed dq-dynamic phasor

The generalised state-space model in (20) can be re-written as:

$$\frac{\mathbf{d}}{\mathbf{dt}}\boldsymbol{\Delta}\mathbf{X_k}=\begin{bmatrix}\mathbf{A-N+\rho} & \mathbf{AC_f} \\ \mathbf{AC_h} & \mathbf{A-N+\rho}\end{bmatrix}\boldsymbol{\Delta}\mathbf{X_k}+\begin{bmatrix}\mathbf{B} & \mathbf{BC} \\ \mathbf{BC} & \mathbf{B}\end{bmatrix}\boldsymbol{\Delta}\mathbf{U_k} \quad (33)$$

where $\mathbf{AC_f}$ and $\mathbf{AC_h}$ are matrices that represent the mutual effect between the fundamental frequency and harmonics, $\boldsymbol{\rho}$ is a diagonal matrix that represents the frequency coupling due to the existence of positive and negative components at a specific frequency, and $\mathbf{N}$ is a diagonal matrix that represents the transformation of differential variables of the system to a dynamic phasor, and is defined as:

$$\mathbf{N}=\mathrm{diag}[0 \quad j\omega I \quad -j\omega I \quad jk_1\omega I \quad -jk_1\omega I \quad \cdots \quad -jk_n\omega I]$$

The eigenvalues of the generalised state matrix in (33) can therefore be written as [45]:

$$\boldsymbol{\lambda}_\mathbf{k}(\mathbf{A_{DP}})=\det(\mathbf{A_{DP}}-\boldsymbol{\lambda})=(\mathbf{A}-\mathbf{N})+\boldsymbol{\rho}\pm(\mathbf{AC_f}.\mathbf{AC_h})^{\frac{1}{2}} \quad (34)$$

According to (34), the inclusion of harmonics in a stable system generates repeated eigenvalues if the coupling term $\{\boldsymbol{\rho}\pm(\mathbf{AC_f}.\mathbf{AC_h})^{\mathbf{1/2}}\}$ is equal to zero. This coupling term has a vital effect on representing different operating conditions of the devices, as the existence of harmonics will be seen as a change of this term.

System stability is ensured when the system eigenvalues ($\boldsymbol{\lambda}_\mathbf{k}$) satisfies:

$$\boldsymbol{\lambda}_\mathbf{k}(\mathbf{A_{DP}})<0 \qquad (-\infty\le\omega\le\infty) \quad (35)$$

The small-signal impedance facilitates stability assessment of the device at the point of common coupling (PCC) using generalised Nyquist stability criterion [46] [47], which plots the eigenvalues of the return ratio matrix ($\mathbf{L_R}$) as:

$$\boldsymbol{\Delta\lambda}_\mathbf{k}=\det(\boldsymbol{\lambda}_\mathbf{k}\mathbf{I}-\langle\mathbf{L_R}\rangle_\mathbf{k})=0 \quad (36)$$

$$\langle\mathbf{L_R}\rangle_k=\langle\mathbf{Z_g}\rangle_\mathbf{k}.\langle\mathbf{Y_{device}}\rangle_\mathbf{k} \quad (37)$$

where $\langle\mathbf{Z_g}\rangle_\mathbf{k}$ and $\langle\mathbf{Y_{device}}\rangle_\mathbf{k}$ are the grid impedance and device admittance in dq-dynamic phasor form as seen from the PCC. Similar to the eigenvalue analysis, when harmonic coupling is ignored the Nyquist contour repeats itself as frequency increases.

6. Stability assessment of test system using generalised models

This section presents four case studies to demonstrate the effectiveness and capacity of the proposed generalised model

when predicting system stability under balanced and unbalanced conditions. The test system parameters and initial operating conditions are listed in Table1.

TABLE 1 TEST SYSTEM PARAMETERS.

Parameter	Value	Parameter	Value
S_{base}	100kVA	K_{ipdq} , K_{iidq}	1000V/A, 400V/A.s
V_{base}	415kV	K_{pvd} , K_{ivd}	20A/V, 200A/V.s
v_{dc}	1000V	K_{pvq}, K_{ivq}	-0.002A/VA,-0.1A/VA.s
C_{dc}	400μF	R_g, L_g	0.25Ω, 1mH
P_L , Q_L	65kW, 12kVAr	R_f , L_f	0.1Ω, 5mH

6.1. Synchronous dq model validation

This section investigates the validity of the benchmark synchronous dq model. A step change in the reactive power reference, from -12kVAr to +12kVAr, is applied at t=0.4s. The dominant eigenvalues of the model at (-2.5+j0.00) are repeated and real, as shown in Table 2, and represent the states of the direct (i_{sd}) and quadrature (i_{sq}) currents. The current settling time is 1.6s. As shown in Fig.3, both currents settle at t=2.0s, validating the benchmark model.

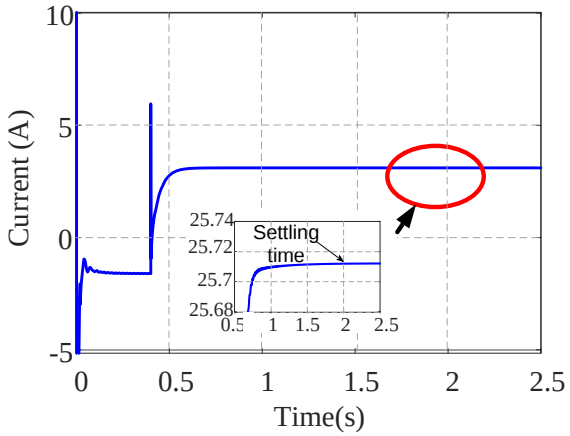

(a)

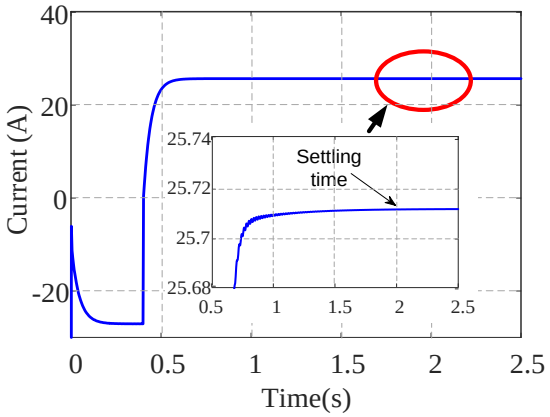

(b)

Fig. 3. Validation of synchronous dq STATCOM model: **(a)** Direct current (i_{sd}), **(b)** Quadrature current (i_{sq}).

6.2. Balanced STATCOM operation with no harmonics

This case study represents a base case and assumes the STATCOM operates under balanced conditions with no harmonics, which is equivalent to $k = 0$ in the proposed generalised model. Table 2 shows that under balanced conditions the test system has seven non-oscillatory stable modes, all located on the left-hand side of the complex plane. The Bode plots of STATCOM impedances for the balanced case are depicted by the solid (blue) line in Fig. . This case study will be used as a benchmark for the following cases to represent the effect of the unbalance and harmonics on STATCOM response.

6.3. Unbalanced STATCOM operation

This section assesses STATCOM stability when it operates in an unbalanced ac grid using generalised state-space and impedance models established in Section 5. The unbalanced voltage waveforms of the STATCOM are shown in Fig.4. The analysis in Table 2 shows eigenvalues for two balanced positive and negative sequence systems, with each system having 7 modes in comparison with balanced system. The positive sequence, which physically rotates at $+\omega_n$, appears at zero frequency because of the frequency shift of the dynamic phasor. The negative sequence which normally rotates at $-\omega_n$ appears at $2\omega_n$ (628.32 Hz). As previously stated in (33), under unbalanced conditions the coupling term $\mathbf{AC_h}$ exists. Note that under unbalanced conditions the negative real parts of the eigenvalues exhibit slight shifts compared to the balanced case.

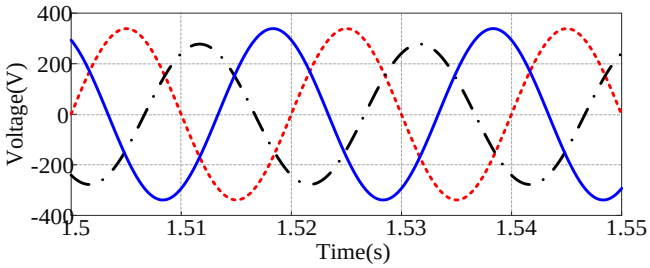

Fig. 4. STATCOM voltage under unbalanced operation

TABLE 2 EIGENVALUE ANALYSIS OF BALANCED AND UNBALANCED TEST SYSTEM

Modes	Balanced condition	Unbalanced condition
λ_1	-1.54×10^5+j0.00	-1.49×10^5+j0.00
λ_2	-7.99×10^4+j0.00	-7.99×10^4+j0.00
λ_3	-221.58+j0.00	-204.51+j0.00
λ_4	-10.47+j0.00	-10.52+j0.00
λ_5	-24.04+j0.00	-23.09+j0.00
λ_6	-2.50+j0.00	-2.50+j0.00
λ_7	-2.50+j0.00	-2.50+j0.00
λ_8		-1.49×10^5+j628.32
λ_9		-7.99×10^4+j628.32
λ_{10}		-204.51+j628.32
λ_{11}		-10.52+j628.32
λ_{12}		-23.09+j628.32
λ_{13}		-2.50+j628.32
λ_{14}		-2.50+j628.32

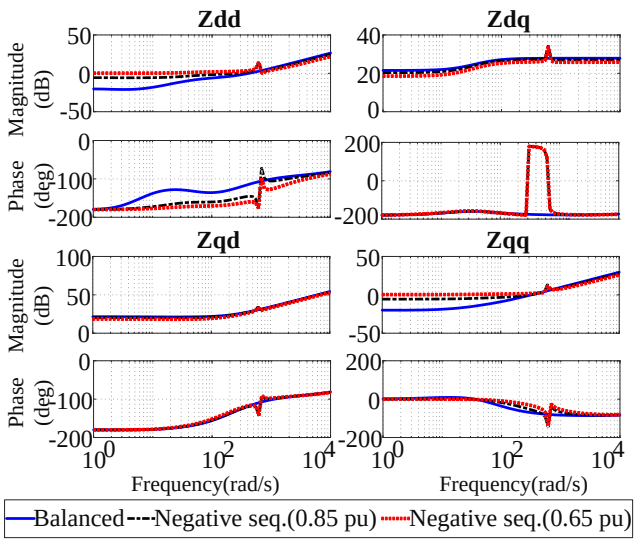

Fig. 5. STATCOM impedance under unbalanced operation.

Fig. shows Bode plots of STATCOM impedances when the phase 'b' voltage is artificially sets as $|V_b| = [1.0 \quad 0.85 \quad 0.65]$ p.u. to reflect voltage unbalance of different severities. As shown in Fig. , the magnitude of the STATCOM negative sequence impedance increases for the diagonal impedance ($\mathbf{Z_{dd}}$ and $\mathbf{Z_{qq}}$) as voltage unbalance severity increases, whilst the diagonal positive sequence impedance remains unchanged. The phase plots also exhibit some differences between balanced and unbalanced conditions. This is related to the coupling present between the fundamental frequency and the negative sequence component. The two impedances at $k = 0,-2$ match each other under balanced operation (with no harmonics) or when the coupling effect is ignored. This can be used to identify the unbalance of the modelled systems which depends on the severity of the unbalance. In summary, the stability assessment under unbalanced operation shows additional eigenvalues, with real parts identical to those of the balanced system and imaginary parts shifted to the double power frequency, resembling the co-existence of positive and negative components. The impedance plots exhibit clear divergence between balanced and unbalanced cases.

6.4. STATCOM operation with harmonics

Assessment of STATCOM operation in the presence of harmonics is facilitated by injection of the 5th and 7th harmonics into the ac grid. These harmonics commonly exist in power networks, particularly, at distribution levels. The STATCOM voltage waveform is presented in Fig.6.

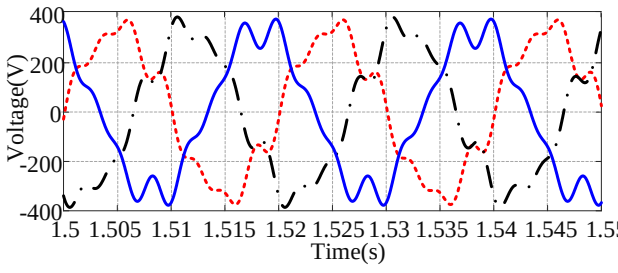

Fig. 6. STATCOM voltage waveform with harmonics

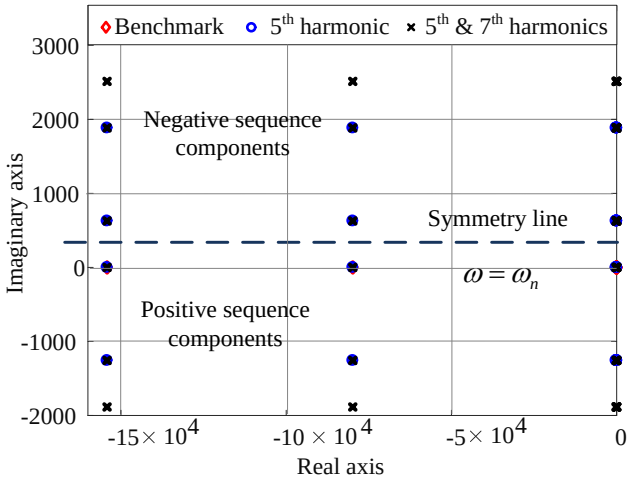

(a)

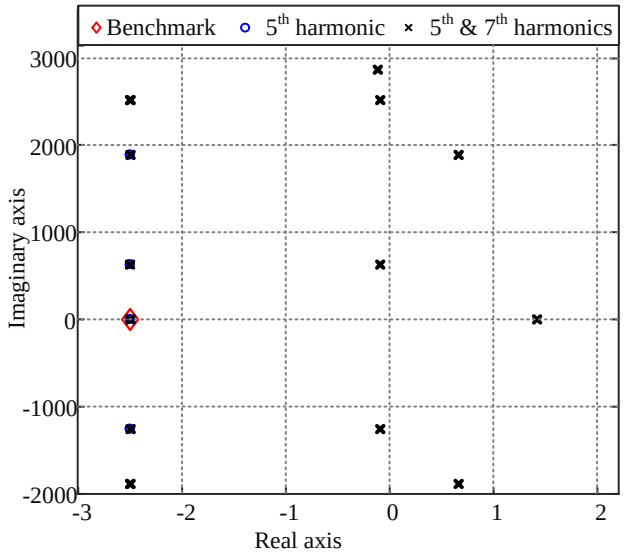

(b)

Fig. 7. Eigenvalue analysis of STATCOM using dq-dynamic phasor: **(a)** Coupling effect ignored, **(b)** Coupling effect considered.

According to (3), transformation of these frequencies to dq-dynamic phasor representation generates six additional frequencies components, which are interpreted as positive and negative sequence components $k - 1 = (1,-1,5,-5,7,-7)$. This case generates 42 eigenvalues, which are shifted up by ω due to the dq-dynamic phasor transformation and not presented as complex conjugates. Thus, the axis of symmetry is located at $\omega = \omega_n$ as shown in Fig.7(a).

The eigenvalues corresponding to positive and negative sequence harmonics are located in the upper and lower parts of the complex plane respectively. The eigenvalues associated with fundamental frequency are real. Fig.7(a) shows that when frequency coupling is ignored the eigenvalues are repeated as multiples of the fundamental frequency. When frequency coupling is considered the eigenvalues are no longer repeated (shifted by ω) as shown in Fig.7(b), where the most dominant eigenvalues are presented. The eigenvalues show the system has become unstable.

Similarly, impedance analysis shows that the inclusion of frequency coupling affects the magnitude and phase of the diagonal STATCOM impedances as shown in Fig.8. When the frequency coupling is ignored the Bode plots of the diagonal STATCOM impedances for different harmonics coincide, whilst they diverge when frequency coupling is considered. Therefore, ignoring the frequency coupling can lead to some errors in stability analysis as the stability norms will be affected by the drift in the magnitudes of impedances of the system being assessed.

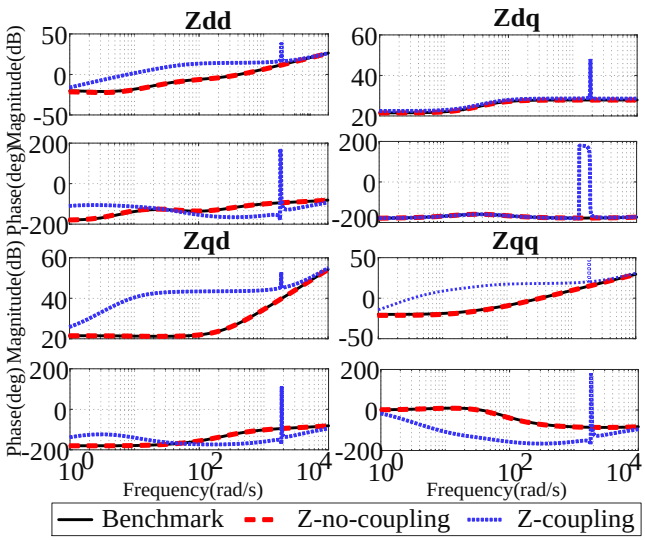

Fig.8. The effect of coupling on STATCOM impedance.

7. Comparison of proposed dq-dynamic phasor and conventional modelling approaches

This section presents high-level comparisons between the proposed dynamic phasor modelling method and several conventional modelling techniques being used for system stability assessment. Table 3 summarises the key attributes and limitations of the modelling approaches being compared.

The synchronous dq modelling method has been adopted as a benchmark against which the proposed extended models are validated. The proposed modelling method shows advantages relative to its counterparts in terms of ability to facilitate more generic stability studies that include a number of harmonics and in unbalanced grids, to cater for harmonic coupling, and to retain the main attributes of linear time invariant systems. The stability criteria of the proposed method can be derived based on the synchronous dq approach due to the similarity between the parameters of both modelling techniques. However, the complexity of the derivation is the main disadvantage. It should be stressed that the selection of modelling approach must be made based on the purpose of the studies to be carried out, taking into account the effort, time and complexity of implementations.

8. Conclusion

A generalised dq-dynamic phasor model and its impedance equivalent are proposed. A STATCOM connected to a grid is employed to demonstrate the effectiveness of the proposed models when assessing the stability of complex power systems that include balanced and unbalanced grids, and a number of harmonics. The proposed modelling method is generalised and validated using MATLAB-Simulink. It is shown that the proposed model can perform stability studies in systems that include harmonic coupling. This is not possible with the LTI-harmonic linearisation method and unified modelling technique. However, the complexity of the derivation could limit the use of this method when analysing large systems. Despite the aforementioned limitations, the proposed generalised model is well-suited for detailed stability assessments of power electronic systems and their control with time constants spread over wide frequency range, encompassing both electromechanical dynamics and electromagnetic transients. Further work on application of the proposed generalised model for development of an arbitrary harmonic suppressor are underway.

TABLE 3 COMPARISON BETWEEN PROPOSED DQ-DYNAMIC PHASOR MODEL AND OTHER MODELLING TECHNIQUES

Characteristic	Identify harmonic effects	Complexity of derivation	Matrices size of each state variable	Identify unbalance	Type of parameters	Stability assessment range
Synchronous dq [7][48]	Multiple coordinates required	Simple	Small	Using (2nd) order harmonic	Linear time-invariant	$(-\infty,+\infty)$
Unified modelling using αβ [16]	Multiple coordinates required	Simple	Small	Limited for $\omega_s > 2\omega_n$	Linear time-variant	$(-\infty,+\infty)$
Single phase dynamic phasor [36], [49], [50]	Not applicable	Simple	Small	Not applicable	Linear time-invariant	$(-\infty,+\infty)$
Harmonics linearisation method-LTI [21][22]	Yes	Moderate	Moderate	Positive negative components	Linear time-invariant	$(-\infty,+\infty)$
Harmonic state-space (HSS) [5] [32]	Yes	Difficult	Large	Positive negative components	Linear time-variant	$(-\frac{\omega_n}{2},+\frac{\omega_n}{2})$
Proposed dq-dynamic phasor	Yes	Difficult	Moderate $(2/3)$ of HSS	Positive negative parameters	Linear time-invariant	$(-\infty,+\infty)$

References

[1] N. Prabhu, M. Janaki, and R. Thirumalaivasan, "Damping of subsynchronous resonance by subsynchronous current injector with STATCOM," *IEEE Reg. 10 Annu. Int. Conf. Proceedings/TENCON*, pp. 1–6, 2009.

[2] X. Wang, F. Blaabjerg, and W. Wu, "Modeling and analysis of harmonic stability in an AC power-electronics- based power system," *IEEE Trans. Power Electron.*, vol. 29, no. 12, pp. 6421–6432, 2014.

[3] A. E. Leon and J. A. Solsona, "Sub-synchronous interaction damping control for DFIG wind turbines," *IEEE Trans. Power Syst.*, vol. 30, no. 1, pp. 419–428, 2015.

[4] A. Moharana and R. K. Varma, "Subsynchronous resonance in single-cage self-excited-induction-generator-based wind farm connected to series-compensated lines," *IET Gener. Transm. Distrib.*, vol. 5, no. 12, pp. 1221–1232, 2011.

[5] M. Hwang and A. Wood, "A new modelling framework for power supply networks with converter based loads and generators-the Harmonic State-Space," *IEEE Int. Conf. Power Syst. Technol.*, pp. 1–6, 2012.

[6] J. Kwon, X. Wang, C. L. Bak, and F. Blaabjerg, "Harmonic interaction analysis in grid connected converter using harmonic state space (HSS) modeling," *Conf. Proc. - IEEE Appl. Power Electron. Conf. Expo. - APEC*, vol. 2015–May, no. May, pp. 1779–1786, 2015.

[7] M. Amin and M. Molinas, "Small-Signal Stability Assessment of Power Electronics Based Power Systems: A Discussion of Impedance-and Eigenvalue-Based Methods," *IEEE Trans. Ind. Appl.*, vol. 53, no. 5, pp. 5014–5030, 2017.

[8] X. Li, G. Zhu, J. Tang, Y. Li, H. Tang, and Y. Huang, "Research on DC-link voltage stabiliser for voltage source converter as connected to weak grid," *J. Eng.*, vol. 2017, no. 13, pp. 2168–2172, 2017.

[9] H. Liu, X. Xie, Y. Li, H. Liu, and Y. Hu, "A small-signal impedance method for analyzing the SSR of series-compensated DFIG-based wind farms," *IEEE Power Energy Soc. Gen. Meet.*, vol. 2015–Septe, 2015.

[10] Y. Liao, Z. Liu, G. Zhang, and C. Xiang, "Vehicle-grid system stability analysis considering impedance specification based on norm criterion," in *2016 IEEE Transportation Electrification Conference and Expo, Asia-Pacific, ITEC Asia-Pacific*, 2016, pp. 118–123.

[11] C. Li, R. Burgos, Y. Tang, and D. Boroyevich, "Impedance-based stability analysis of multiple STATCOMs in proximity," in *2016 IEEE 17th Workshop on Control and Modeling for Power Electronics, COMPEL 2016*, 2016, pp. 1–6.

[12] B. Wen, D. Boroyevich, P. Mattavelli, R. Burgos, and Z. Shen, "Modeling the output impedance negative incremental resistance behavior of grid-tied inverters," in *Conference Proceedings - IEEE Applied Power Electronics Conference and Exposition - APEC*, 2014, pp. 1799–1806.

[13] F. Feng, F. Wu, and H. B. Gooi, "Small Signal Impedance Model and Stability Analysis of Bidirectional Two-Stage DC-DC-AC System," *2017 IEEE 3rd Int. Futur. Energy Electron. Conf. ECCE Asia (IFEEC 2017 - ECCE Asia)*, pp. 1817–1821, Jun. 2017.

[14] B. Wen, D. Dong, D. Boroyevich, R. Burgos, P. Mattavelli, and Z. Shen, "Impedance-based analysis of grid-synchronization stability for three-phase paralleled converters," *IEEE Trans. Power Electron.*, vol. 31, no. 1, pp. 26–38, Jan. 2016.

[15] H. Yang and H. Nian, "Stability analysis of grid-connected converter based on interconnected system impedance modeling under unbalanced grid conditions," *2014 17th Int. Conf. Electr. Mach. Syst. ICEMS 2014*, pp. 2631–2636, 2015.

[16] X. Wang, L. Harnefors, and F. Blaabjerg, "Unified Impedance Model of Grid-Connected Voltage-Source Converters," *IEEE Trans. Power Electron.*, vol. 33, no. 2, pp. 1775–1787, 2018.

[17] M. Cespedes and J. Sun, "Impedance modeling and analysis of grid-connected voltage-source converters," *IEEE Trans. Power Electron.*, vol. 29, no. 3, pp. 1254–1261, Mar. 2014.

[18] M. K. Bakhshizadeh, X. Wang, F. Blaabjerg, J. Hjerrild, L. Kocewiak, C. L. Bak, and B. Hesselbak, "Couplings in Phase Domain Impedance Modeling of Grid-Connected Converters," *IEEE Trans. Power Electron.*, vol. 31, no. 10, pp. 6792–6796, 2016.

[19] A. Rygg, M. Molinas, C. Zhang, and X. Cai, "A Modified Sequence-Domain Impedance Definition and Its Equivalence to the dq-Domain Impedance Definition for the Stability Analysis of AC Power Electronic Systems," *IEEE J. Emerg. Sel. Top. Power Electron.*, vol. 4, no. 4, pp. 1383–1396, 2016.

[20] X. Wang and F. Blaabjerg, "Harmonic Stability in Power Electronic Based Power Systems: Concept, Modeling, and Analysis," *IEEE Trans. Smart Grid*, vol. 3053, no. c, pp. 1–12, 2018.

[21] H. Liu and J. Sun, "Modeling and analysis of DC-link harmonic instability in LCC HVDC systems," *2013 IEEE 14th Work. Control Model. Power Electron. COMPEL 2013*, no. Lcc, 2013.

[22] T. Li, A. M. Gole, and C. Zhao, "Harmonic Instability in MMC-HVDC Converters Resulting from Internal Dynamics," *IEEE Trans. Power Deliv.*, vol. 31, no. 4, pp. 1738–1747, 2016.

[23] Y. Wang, X. Chen, Y. Zhang, J. Chen, and C. Gong, "Impedance modeling of three-phase grid-connected inverters and analysis of interaction stability in grid-connected system," in *2016 IEEE 8th International Power Electronics and Motion Control Conference, IPEMC-ECCE Asia 2016*, 2016, pp. 3606–3612.

[24] Y. Cen, M. Huang, and X. Zha, "Modeling method of sequence admittance for three-phase voltage source converter under unbalanced grid condition," *J. Mod. Power Syst. Clean Energy*, vol. 6, no. 3, pp. 595–606, 2018.

[25] S. Filizadeh and A. M. Gole, "Harmonic Performance Analysis of an OPWM-Controlled STATCOM in Network Applications," *IEEE Trans. Power Deliv.*, vol. 20, no. 2, pp. 1001–1008, Apr. 2005.

[26] X.-D. Chen, S.-R. Yu, and X.-L. Ge, "Modelling and stability analysis of virtual synchronous machine using harmonic state-space modelling method," *J. Eng.*, 2018.

[27] R. Z. Scapini, L. V. Bellinaso, and L. Michels, "Stability analysis of half-bridge rectifier employing LTP approach," *IECON Proc. (Industrial Electron. Conf.*, pp. 780–785, 2012.

[28] N. M. Wereley and S. R. Hall, "Frequency response of linear time periodic systems," *Proc. 29th IEEE Conf. Decis. Control*, vol. 6, pp. 3650–3655, 1990.
[29] İ. Uyanık, M. M. Ankaralı, N. J. Cowan, Ö. Morgül, and U. Saranlı, "Identification of a Hybrid Spring Mass Damper via Harmonic Transfer Functions as a Step Towards Data-Driven Models for Legged Locomotion," Jan. 2015.
[30] V. Salis, A. Costabeber, S. M. Cox, and P. Zanchetta, "Stability assessment of power-converter-based AC systems by LTP theory: Eigenvalue analysis and harmonic impedance estimation," *IEEE J. Emerg. Sel. Top. Power Electron.*, vol. 5, no. 4, pp. 1513–1525, 2017.
[31] W. Xu, J. E. Drakos, Y. Mansour, A. Chang, and B. C. Hydro, "A three-phase converter model for harmonic analysis of HVDC systems," *IEEE Trans. Power Deliv.*, vol. 9, no. 3, pp. 1724–1731, 1994.
[32] J. Kwon, X. Wang, F. Blaabjerg, C. L. Bak, V. S. Sularea, and C. Busca, "Harmonic Interaction Analysis in a Grid-Connected Converter Using Harmonic State-Space (HSS) Modeling," *IEEE Trans. Power Electron.*, vol. 32, no. 9, pp. 6823–6835, 2017.
[33] S. R. Sanders, J. M. Noworolski, X. Z. Liu, and G. C. Verghese, "Generalized Averaging Method for Power Conversion Circuits," *IEEE Trans. Power Electron.*, vol. 6, no. 2, pp. 333–340, 1991.
[34] M. Parimi, M. Monika, M. Rane, S. Wagh, and A. Stankovic, "Dynamic phasor-based small-signal stability analysis and control of solid state transformer," *2016 IEEE 6th Int. Conf. Power Syst. ICPS 2016*, 2016.
[35] M. C. Chudasama and A. M. Kulkarni, "Dynamic phasor analysis of SSR mitigation schemes based on passive phase imbalance," *IEEE Trans. Power Syst.*, vol. 26, no. 3, pp. 1668–1676, 2011.
[36] L. Piyasinghe, Z. Miao, J. Khazaei, L. Fan, Zhixin Miao, J. Khazaei, Lingling Fan, Z. Miao, J. Khazaei, L. Fan, S. Member, J. Khazaei, L. Fan, S. Member, Zhixin Miao, J. Khazaei, Lingling Fan, Z. Miao, J. Khazaei, and L. Fan, "Impedance model-based SSR analysis for TCSC compensated type-3 wind energy delivery systems," *IEEE Trans. Sustain. Energy*, vol. 6, no. 1, pp. 179–187, Jul. 2015.
[37] Z. Shuai, Y. Peng, J. M. Guerrero, Y. Li, and J. Z. Shen, "Transient Response Analysis of Inverter-based Microgrids under Unbalanced Conditions using Dynamic Phasor Model," *IEEE Trans. Ind. Electron.*, vol. 0046, no. c, pp. 1–11, 2018.
[38] K. Abojlala, D. Holliday, and L. Xu, "Transient analysis of an interline dynamic voltage restorer using dynamic phasor representation," in *2016 IEEE 17th Workshop on Control and Modeling for Power Electronics, COMPEL 2016*, 2016, pp. 1–7.
[39] L. Harnefors, "Analysis of subsynchronous torsional interaction with power electronic converters," *IEEE Trans. Power Syst.*, vol. 22, no. 1, pp. 305–313, Feb. 2007.
[40] X. Lombard and P. G. Therond, "Control of unified power flow controller: Comparison of methods on the basis of a detailed numerical model," *IEEE Trans. Power Syst.*, vol. 12, no. 2, pp. 824–830, 1997.
[41] Y. Familiant, K. Corzine, J. Huang, and M. Belkhayat, "AC Impedance Measurement Techniques," *IEEE Int. Conf. Electr. Mach. Drives, 2005.*, pp. 1850–1857, 2005.
[42] K. Abojlala, D. Holliday, and L. Xu, "Stability norms control using the virtual impedance concept for power frequency applications," in *19th International Symposium on Power Electronics, Ee 2017*, 2017, vol. 2017–Decem, pp. 1–6.
[43] N. Flourentzou and V. G. Agelidis, "Optimized modulation for ACDC harmonic immunity in VSC HVDC transmission," *IEEE Trans. Power Deliv.*, vol. 25, no. 3, pp. 1713–1720, 2010.
[44] J. R. C. Orillaza and A. R. Wood, "Harmonic state-space model of a controlled TCR," *IEEE Trans. Power Deliv.*, vol. 28, no. 1, pp. 197–205, 2013.
[45] N. M. Wereley, "Analysis and control of linear periodically time varying systems," Massachusetts Institute of Technology, Dept. of Aeronautics and Astronautics, 1990.
[46] J. Huang, K. A. Corzine, and M. Belkhayat, "Small-signal impedance measurement of power-electronics-based AC power systems using line-to-line current injection," *IEEE Trans. Power Electron.*, vol. 24, no. 2, pp. 445–455, 2009.
[47] M. K. Das, A. M. Kulkarni, and P. B. Darji, "Comparison of DQ and Dynamic Phasor based frequency scanning analysis of grid-connected Power Electronic Systems," *19th Power Syst. Comput. Conf. PSCC 2016*, no. 1, 2016.
[48] S. Skogestad, I. Postelthwaite, I. Postlethwaite, I. P. Sigurd Skogestad, and I. Postelthwaite, *Multivariable feedback control: analysis and design*, vol. 8, no. 14. John Wiley, 2005.
[49] S. Lissandron, L. Dalla Santa, P. Mattavelli, and B. Wen, "Validation of impedance-based small-signal stability analysis for single-phase grid-feeding inverters with PLL," *2015 IEEE 6th Int. Symp. Power Electron. Distrib. Gener. Syst. PEDG 2015*, 2015.
[50] G. N. Love and a. R. Wood, "Harmonic State Space model of power electronics," *2008 13th Int. Conf. Harmon. Qual. Power*, vol. 1, pp. 2–7, 2008.

Appendix

Generalised state-space model

$$\mathbf{a_{k,k}}=\begin{bmatrix} -jk\omega & 0 & K_{iid} & 0 & -K_{iid} & 0 & -K_{iid}K_{pvd} \\ 0 & -jk\omega & 0 & K_{iiq} & -\frac{3}{2}K_{iiq}K_{pvq}\langle v_{sq}\rangle_0 & \frac{3}{2}K_{iiq}K_{pvq}\langle v_{sd}\rangle_0 - K_{iiq} & 0 \\ 0 & 0 & -jk\omega & 0 & 0 & 0 & -K_{ivd} \\ 0 & 0 & 0 & -jk\omega & -\frac{3}{2}K_{ivq}\langle v_{sq}\rangle_0 & \frac{3}{2}K_{ivq}\langle v_{sd}\rangle_0 & 0 \\ \frac{1}{L_f} & 0 & \frac{Kp_{id}}{L_f} & 0 & \frac{-R_f-K_{pid}}{L_f}-jk\omega & \omega & \frac{-K_{pid}K_{pvd}}{L_f} \\ 0 & \frac{1}{L_f} & 0 & \frac{Kp_{iq}}{L_f} & -\omega-\frac{\frac{3}{2}K_{piq}K_{pvq}\langle v_{sq}\rangle_0}{L_f} & \frac{\frac{3}{2}K_{piq}K_{pvq}\langle v_{sd}\rangle_0-R_f-K_{piq}}{L_f}-jk\omega & 0 \\ 0 & 0 & 0 & 0 & \alpha_1 & \alpha 2 & \alpha 3-jk\omega \end{bmatrix}$$

$$\alpha_1=\tfrac{3}{2}\sum_i^{k=0}\langle\tfrac{1}{C_{dc}v_{dc}}\rangle_{k-i}\langle v_{sd}\rangle_i-\sum_i^{k=0}\langle\tfrac{1}{C_{dc}v_{dc}}\rangle_{k-i}\langle 2R_fi_{sd}\rangle_i\ \alpha 2=\tfrac{3}{2}\sum_i^{k=0}\langle\tfrac{1}{C_{dc}v_{dc}}\rangle_{k-i}\langle v_{sq}\rangle_i$$
$$\alpha 3=\sum_i^{k=0}\langle\tfrac{1}{C_{dc}v_{dc}^2}\rangle_{k-i}\langle i_{sd}^2.R_f\rangle_i-\tfrac{3}{2}\sum_i^{k=0}\langle\tfrac{1}{C_{dc}v_{dc}^2}\rangle_{k-i}\langle v_{sd}i_{sd}\rangle_i-\tfrac{3}{2}\sum_i^{k=0}\langle\tfrac{1}{C_{dc}v_{dc}^2}\rangle_{k-i}\langle v_{sq}.i_{sq}\rangle_i$$

$$\mathrm{ac_{k=k}}=\begin{bmatrix} 0 & 0 & 0 \\ -\frac{3}{2}K_{iiq}K_{pvq}\langle v_{sq}\rangle_{-k} & \frac{3}{2}K_{iiq}K_{pvq}\langle v_{sd}\rangle_{-k} & 0 \\ 0 & 0 & 0 \\ -\frac{3}{2}K_{ivq}\langle v_{sq}\rangle_{-k} & \frac{3}{2}K_{ivq}\langle v_{sd}\rangle_{-k} & 0 \\ 0 & 0 & 0 \\ -\frac{3}{2}\frac{K_{piq}K_{pvq}\langle v_{sq}\rangle_{-k}}{L_f} & -\frac{3}{2}\frac{K_{piq}K_{pvq}\langle v_{sd}\rangle_{-k}}{L_f} & 0 \\ \alpha 4 & \alpha 5 & \alpha 6 \end{bmatrix}\begin{matrix} \alpha 4=\frac{3}{2}\sum_i^{k=\bar{k}}\langle\frac{1}{C_{dc}v_{dc}}\rangle_{k-i}\langle v_{sd}\rangle_i- \\ \sum_i^{k=\bar{k}}\langle\frac{1}{C_{dc}v_{dc}}\rangle_{k-i}\langle 2R_fi_{sd}\rangle_i \\ \alpha 5=\frac{3}{2}\sum_i^{k=\bar{k}}\langle\frac{1}{C_{dc}v_{dc}}\rangle_{k-i}\langle v_{sq}\rangle_i \\ \alpha 6=\sum_i^{k=\bar{k}}\langle\frac{1}{C_{dc}v_{dc}^2}\rangle_{k-i}\langle i_{sd}^2.R_f\rangle_i- \\ \frac{3}{2}\sum_i^{k=\bar{k}}\langle\frac{1}{C_{dc}v_{dc}^2}\rangle_{k-i}\langle v_{sd}\,i_{sd}\rangle_i- \\ \frac{3}{2}\sum_i^{k=\bar{k}}\langle\frac{1}{C_{dc}v_{dc}^2}\rangle_{k-i}\langle v_{sq}.i_{sq}\rangle_i \end{matrix}$$

$$\mathbf{B_{k,k}}=\begin{bmatrix} 0 & 0 & K_{iid}K_{pvd} & 0 \\ \frac{3}{2}K_{iiq}K_{pvq}\langle i_{sq}\rangle_0 & -\frac{3}{2}K_{iiq}K_{pvq}\langle i_{sd}\rangle_0 & 0 & K_{iiq}K_{pvq} \\ 0 & 0 & Ki_{vd} & 0 \\ \frac{3}{2}K_{ivq}\langle i_{sq}\rangle_0 & -\frac{3}{2}K_{ivq}\langle i_{sd}\rangle_0 & 0 & K_{ivq} \\ \frac{1}{L_f} & 0 & \frac{K_{pid}K_{pvd}}{L_f} & 0 \\ \frac{3}{2}\frac{K_{piq}K_{pvq}\langle i_{sq}\rangle_0}{L_f} & \frac{1}{L_f}-\frac{3}{2}\frac{K_{piq}K_{pvq}\langle i_{sd}\rangle_0}{L_f} & 0 & \frac{K_{piq}K_{pvq}}{L_f} \\ \frac{3}{2}\langle\frac{i_{sd}}{C_{dc}v_{dc}}\rangle_0 & \frac{3}{2}\langle\frac{i_{sq}}{C_{dc}v_{dc}}\rangle_0 & 0 & 0 \end{bmatrix}\quad \mathrm{bc_{k=k}}=\begin{bmatrix} 0 & 0 & 0\ 0 \\ -\frac{3}{2}K_{iiq}K_{pvq}\langle i_{sq}\rangle_{-k} & \frac{3}{2}K_{iiq}K_{pvq}\langle i_{sd}\rangle_{-k} & 0\ 0 \\ 0 & 0 & 0\ 0 \\ -\frac{3}{2}K_{ivq}\langle i_{sq}\rangle_{-k} & \frac{3}{2}K_{ivq}\langle i_{sd}\rangle_{-k} & 0\ 0 \\ 0 & 0 & 0\ 0 \\ -\frac{3}{2}\frac{K_{piq}K_{pvq}\langle i_{sq}\rangle_{-k}}{L_f} & -\frac{3}{2}\frac{K_{piq}K_{pvq}\langle i_{sd}\rangle_{-k}}{L_f} & 0\ 0 \\ \frac{3}{2}\langle\frac{i_{sd}}{C_dv_{dc}}\rangle_{-k} & \frac{3}{2}\langle\frac{i_{sq}}{C_{dc}v_{dc}}\rangle_{-k} & 0\ 0 \end{bmatrix}$$

Generalised Impedance model

$$\mathbf{hd_k}=\begin{bmatrix} L_f(s+jk\omega)+R_f-\langle k_{pid}+\frac{K_{iid}}{s}\rangle_0 & -\omega L_f \\ \omega L_f & L_f(s+jk\omega)+R_f-\langle K_{piq}+\frac{K_{iiq}}{s}\rangle_0 \end{bmatrix}\ \mathbf{hl_{k=k}}=\begin{bmatrix} -\langle\frac{K_{iid}}{s+jk\omega}\rangle_k & 0 \\ 0 & -\langle\frac{K_{iiq}}{s+jk\omega}\rangle_k \end{bmatrix}\ \mathbf{Dd_k}=\begin{bmatrix}\alpha l_k & 0\\ 0 & 1\end{bmatrix}$$

$$\mathbf{Bd_k}=\begin{bmatrix}\langle k_{pid}+\frac{K_{iid}}{s}\rangle_0 & 0\\ 0 & \langle K_{piq}+\frac{K_{iiq}}{s}\rangle_0\end{bmatrix}\ \mathbf{Fd_k}=\begin{bmatrix}\left(\langle\frac{3}{2}v_{sd}\rangle_0-\langle 2R_fi_{sd}\rangle_0\right) & \langle\frac{3}{2}v_{sq}\rangle_0\\ \frac{3}{2}\langle v_{sq}\rangle_0 & -\frac{3}{2}\langle v_{sd}\rangle_0\end{bmatrix}\ \mathbf{Bl_{k=k}}=\begin{bmatrix}\langle\frac{Ki_{id}}{s+jk\omega}\rangle_k & 0\\ 0 & \langle\frac{Ki_{iq}}{s+jk\omega}\rangle_k\end{bmatrix}$$

$$\mathbf{El_{k=k}}=\tfrac{3}{2}\begin{bmatrix}\langle i_{sd}\rangle_k & \langle i_{sq}\rangle_k\\ -\langle i_{sq}\rangle_{k^*} & \langle i_{sd}\rangle_{k^*}\end{bmatrix}\mathbf{Cl_{k=k}}=\begin{bmatrix}\langle\frac{K_{ivd}}{s+jk\omega}\rangle_k & 0\\ 0 & \langle\frac{K_{ivq}}{s+jk\omega}\rangle_k\end{bmatrix}\mathbf{Cd_k}=\begin{bmatrix}K_{pvd}+\langle\frac{K_{ivd}}{s}\rangle_0 & 0\\ 0 & K_{pvq}+\langle\frac{K_{ivq}}{s}\rangle_0\end{bmatrix}\mathbf{Ed_k}=\tfrac{3}{2}\begin{bmatrix}\langle i_{sd}\rangle_0 & \langle i_{sq}\rangle_0\\ -\langle i_{sq}\rangle_0 & \langle i_{sd}\rangle_0\end{bmatrix}$$

$$\mathbf{Fl_{k=k}}=\begin{bmatrix}\langle\frac{3}{2}v_{sd}\rangle_k-\langle 2R_fi_{sd}\rangle_k & \langle\frac{3}{2}v_{sq}\rangle_k\\ \frac{3}{2}\langle v_{sq}\rangle_k & -\frac{3}{2}\langle v_{sd}\rangle_k\end{bmatrix}\ \mathbf{Dl_{k=k}}=\begin{bmatrix}\alpha m_{k=k} & 0\\ 0 & 0\end{bmatrix}$$

$$\alpha l=C_{dc}s\langle v_{dc}\rangle_0-\left(\sum_i^{k=0}\langle\tfrac{1}{v_{dc}}\rangle_{k-i}\langle i_{sd}^2R_f\rangle_i\right)+\tfrac{3}{2}\sum_i^{k=0}\langle\tfrac{1}{v_{dc}}\rangle_{k-i}\langle v_{sd}\rangle_i\langle i_{sd}\rangle_0+\tfrac{3}{2}\sum_i^{k=\bar{k}}\langle\tfrac{1}{v_{dc}}\rangle_{k-i}\langle v_{sd}\rangle_i\langle i_{sd}\rangle_k+$$
$$\tfrac{3}{2}\sum_i^{k=k}\langle\tfrac{1}{v_{dc}}\rangle_{k-i}\langle v_{sd}\rangle_i\langle i_{sd}\rangle_{\bar{k}}+\tfrac{3}{2}\sum_i^{k=0}\langle\tfrac{1}{v_{dc}}\rangle_{k-i}\langle v_{sq}\rangle_i\langle i_{sq}\rangle_0+\tfrac{3}{2}\sum_i^{k=\bar{k}}\langle\tfrac{1}{v_{dc}}\rangle_{k-i}\langle v_{sq}\rangle_i\langle i_{sq}\rangle_k+\tfrac{3}{2}\sum_i^{k=k}\langle\tfrac{1}{v_{dc}}\rangle_{k-i}\langle v_{sq}\rangle_i\langle i_{sq}\rangle_{\bar{k}}$$
$$\alpha m_{k=k}=C_{dc}(s+jk\omega)\langle v_{dc}\rangle_k-\left(\sum_i^{k=k}\langle\tfrac{1}{v_{dc}}\rangle_{k-i}\langle i_{sd}^2R_f\rangle_i\right)+\tfrac{3}{2}\sum_i^{k=0}\langle\tfrac{1}{v_{dc}}\rangle_{k-i}\langle v_{sd}\rangle_i\langle i_{sd}\rangle_k+\tfrac{3}{2}\sum_i^{k=k}\langle\tfrac{1}{v_{dc}}\rangle_{k-i}\langle v_{sd}\rangle_i\langle i_{sd}\rangle_0+$$
$$\tfrac{3}{2}\sum_i^{k=0}\langle\tfrac{1}{v_{dc}}\rangle_{k-i}\langle v_{sq}\rangle_i\langle i_{sq}\rangle_k+\tfrac{3}{2}\sum_i^{k=k}\langle\tfrac{1}{v_{dc}}\rangle_{k-i}\langle v_{sq}\rangle_i\langle i_{sq}\rangle_0$$